

## Synthesis, Spectroscopic Studies, Biological Screening and Geometrical Optimization of Bidentate Schiff's Base Ligand and their Mn(II) and Co(II) Complexes

PALLAVI JAIN<sup>1,\*</sup>, DINESH KUMAR<sup>2</sup> and SULEKH CHANDRA<sup>3</sup>

<sup>1</sup>Department of Chemistry, SRM Institute of Science & Technology, Modinagar-201 204, India

<sup>2</sup>School of Chemical Sciences, Central University of Gujarat, Gandhinagar-382 030, India

<sup>3</sup>Department of Chemistry, Zakir Hussain Delhi College, J.L.N. Marg, New Delhi-110 002, India

\*Corresponding author: E-mail: palli24@gmail.com

Received: 24 March 2018;

Accepted: 23 April 2018;

Published online: 31 May 2018;

AJC-18951

A series of Mn(II) and Co(II) complexes were obtained after the condensation of ligand methylcarbamatesemicarbazone (L) and corresponding metal salt. The ratio of metal salt to ligand was 1:2. The conventional condensation reaction was employed to synthesize the multidonor ligand by refluxing methylcarbamate and semicarbazide in 1:1 ratio. The mode of bonding and geometry of the synthesized complexes was confirmed by elemental analysis, magnetic susceptibility, molar conductance, IR, <sup>1</sup>H NMR, Mass, electronic spectra, EPR and molecular modeling. The general composition ML<sub>2</sub>X<sub>2</sub> was assigned to transition metal complexes, where M = Mn(II) and Co(II), L = methylcarbamatesemicarbazone and X = CH<sub>3</sub>COO<sup>-</sup>, NO<sub>3</sub><sup>-</sup>. The non-electrolytic nature of metal complexes was confirmed by molar conductance values with composition [ML<sub>2</sub>X<sub>2</sub>]. The spectral studies suggested six coordinated geometry for the synthesized complexes. Molecular Modeling of ligand and complexes was also done by using Gaussian. The biological activities of all the synthesized compounds were also evaluated against two different bacterias. Based on antimicrobial results, it was concluded that metal complexes exhibited higher inhibition potential than free Schiff's base ligand.

**Keywords:** Schiff's base ligand, Metal complexes, Spectroscopic, Molecular Modeling, Antimicrobial study.

### INTRODUCTION

Semicarbazones are the derivatives of urea and oxygen-nitrogen based compounds. These semicarbazones are the subject of interest since long time. Semicarbazones are synthesized as a result of condensation reaction of semicarbazones with ketones or aldehydes. The ketones or aldehydes can be aromatic, aliphatic or hetrocyclic. The biological and pharmacological applications of Schiff's base metal complexes of semicarbazone attracted much attention of researchers and scientists in recent years [1,2].

The coordination complexes of semicarbazones with different physical, chemical and structural properties are the subject of interest [3,4]. Interestingly, semicabazone based Schiff's base ligands with N<sub>4</sub> atom substituent are acknowledged for enhancing growth inhibitory activity. The substitution of groups at terminal nitrogen atom complements the biological importance of semicarbazones [5-7]. Semicarbazide compounds also demonstrate an extensive range of biological activities ranging from antimicrobial [8], antiproliferative [9], antitumor [10], anticancer [11], anti-inflammatory [12], antifungal [13], antimalarial [14] and antitrypanosomicidal [15] and anti-

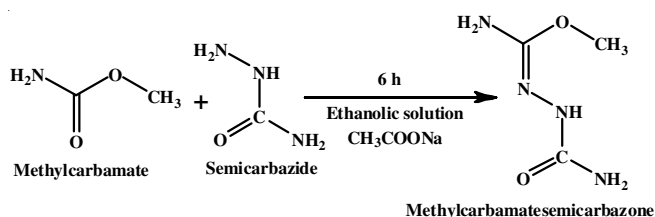
leishmanicidal activities [16]. Semicarbazones are also found to have antitrypanosoma cruzi activity [17]. Moreover, the biological activities of semicarbazone and their metal complexes could be due to metal ion coordination. Semicarbazones are also used as inhibitors in different biological processes such as a Jack bean urease inhibitor [18], c-Met kinase inhibitors [19], inhibitors of cathepsin B, cathepsin H & cathepsin L [20]. In sensing, semicarbazones again found to be active as an ionophore [21]. In keeping view of above biological applications, semicarbazone based Schiff's base ligands and complexes are in great demand. This research paper consists of the synthesis, characterization of semicarbazide based ligand and its Mn(II) and Co(II) complexes. The synthesized nitrogen and oxygen donor atom containing Schiff's base ligand and complexes were also evaluated for the biological activities against some microorganism. Gaussian method was also employed for the computational studies of ligand and its metal complexes.

### EXPERIMENTAL

AR grade chemicals and standard/spectroscopic grades solvents were used in this research work. The chemicals were

purchased from Sigma Aldrich whereas metal salts were purchased from E. Merck.

**Synthesis of ligand:** A hot ethanolic solution of methylcarbamate was added to an aqueous solution of semicarbazide hydrochloride in the presence of sodium acetate in the ration of 1:1:1. The mixture was refluxed at 75 °C for 6 h, over a water condenser. After refluxing, the solution was kept in refrigerator overnight at 0 °C for cooling. A light yellow colour precipitate was appeared. The precipitate was filtered off and washed with cold ethanol and finally dried under vacuum over P<sub>4</sub>O<sub>10</sub> (Scheme-I).



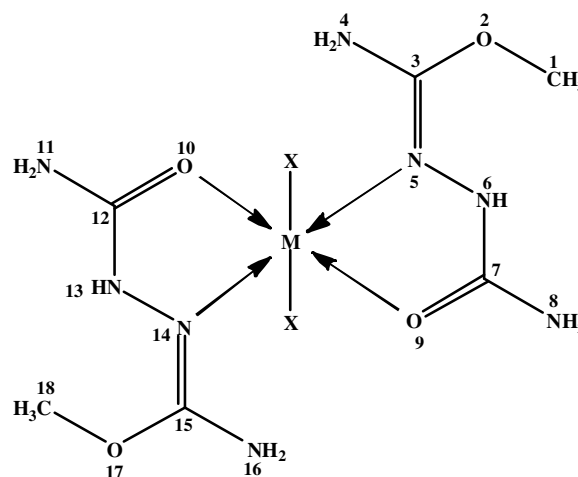
Scheme-I: Synthesis of semicarbazone based Schiff's base ligand

**Synthesis of Mn(II) and Co(II) complexes:** An ethanolic solution of Mn(II) and Co(II) salts of acetate and nitrate was added to a hot ethanolic solution of nitrogen and oxygen atom containing ligand in 1:2 stoichiometry proportion. The solutions so obtained were refluxed at 70-75 °C for 8-11 h. After refluxing, the solutions were cooled by keeping in refrigerator. The different colour precipitates were appeared and filtered off. The obtained precipitates were washed with ethanol and distilled water and finally dried over P<sub>4</sub>O<sub>10</sub> under vacuum.

**Physical measurement:** Carlo-Erba 1106 analyser was employed for the elemental analysis (C, H and N) of ligand and complexes. Molar conductance values were calculated with the help of an ELICO (CM82T) conductivity bridge. Gouy balance was used for the calculation of magnetic susceptibility by using CuSO<sub>4</sub>·5H<sub>2</sub>O as a calibrant at room temperature. Mass spectra were obtained by using JEOL, JMS, DX-303 mass spectrometer. Hitachi FT NMR, model R-600 spectrometer was used to record <sup>1</sup>H NMR spectra using deuteriated CDCl<sub>3</sub> as solvent. Perkin-Elmer FTIR Spectrum BX-II spectrophotometer was employed to obtain IR spectra (KBr). Shimadzu UV mini-1240 spectrophotometer was employed to obtain the electronic spectra in DMSO. E4-EPR spectrometer was employed to record EPR spectra of metal complexes as polycrystalline samples using DPPH as the g-marker.

## RESULTS AND DISCUSSION

A nitrogen and oxygen donor atoms containing bidentate ligand and Mn(II) and Co(II) complexes were synthesized by using conventional condensation method. According to analytical and spectral data, metal complexes possessed the general composition ML<sub>2</sub>X<sub>2</sub>, where X = CH<sub>3</sub>COO<sup>-</sup>, NO<sub>3</sub><sup>-</sup>. Non-electrolytic nature of all the metal complexes was confirmed by molar conductance studies. Table-1 shows the analytical and physical data of the bidentate ligand and complexes. IR spectroscopic analysis confirms the coordination of ligand to metal ion through nitrogen and oxygen donor atoms. Six coordinated octahedral geometry assigned to the synthesized complexes (Fig. 1).



where, M = Mn(II), Co(II) and X = Cl<sup>-</sup>, CH<sub>3</sub>COO<sup>-</sup>

Fig. 1. Proposed structure of metal complex of Schiff's base ligand

**<sup>1</sup>H NMR spectrum of ligand:** <sup>1</sup>H NMR spectrum of ligand containing different signals confirms the existence of three different types of protons. The <sup>1</sup>H NMR spectrum of ligand L was recorded in DMSO-*d*<sub>6</sub>. Tetramethylsilane (TMS) was used as the internal standard. <sup>1</sup>H NMR spectrum of ligand L (400 MHz, DMSO-*d*<sub>6</sub>) shows signals at δ = 8.75 ppm (s, 1H, NH), δ = 6.75 ppm (s, 4H, NH<sub>2</sub>) and δ = 2.49 ppm (s, 3H, -CH<sub>3</sub>) [22].

**Mass spectrum:** The formula weight of the ligand was confirmed by the mass spectrum exhibited the molecular ion peak at *m/z* = 131.54 which corresponds to [C<sub>3</sub>H<sub>8</sub>N<sub>4</sub>O<sub>2</sub>]<sup>+</sup>. The other peaks were appeared at *m/z* = 116.42, 88.67, 59.25, 44.26 and

TABLE-1  
PHYSICAL DATA AND ANALYTICAL PROPERTIES OF LIGAND AND THEIR CORRESPONDING COMPLEXES

Reactant (g)		Molar ratio	Product	Colour	f.w. (g/mol)	Molar cond. (Ω <sup>-1</sup> cm <sup>2</sup> mol <sup>-1</sup> )	Yield (%)	Elemental analysis (%):			
Metal salt	Ligand							Found (calcd.)	C	H	N
Mn(CH <sub>3</sub> COO) <sub>2</sub> ·4H <sub>2</sub> O 1.22	L 1.32	1:2	[Mn(L) <sub>2</sub> (OAc) <sub>2</sub> ] C <sub>10</sub> H <sub>22</sub> N <sub>8</sub> O <sub>8</sub> Mn	Off-White	436.9 [245-247]	0.20	65 [9]	27.45 (27.46)	5.05 (5.03)	25.65 (25.63)	12.51 (12.56)
Mn(NO <sub>3</sub> ) <sub>2</sub> ·H <sub>2</sub> O 0.984	L 1.32	1:2	[Mn(L) <sub>2</sub> (NO <sub>3</sub> ) <sub>2</sub> ] C <sub>6</sub> H <sub>16</sub> N <sub>10</sub> O <sub>10</sub> Mn	White	442.9 [225-228]	0.28	59 [9]	16.30 (16.25)	3.63 (3.61)	31.61 (31.60)	12.40 (12.39)
Co(CH <sub>3</sub> COO) <sub>2</sub> ·H <sub>2</sub> O 0.974	L 1.32	1:2	[Co(L) <sub>2</sub> (OAc) <sub>2</sub> ] C <sub>10</sub> H <sub>22</sub> N <sub>8</sub> O <sub>8</sub> Co	Dark Pink	440.9 [> 300]	0.21	56 [10]	27.20 (27.21)	5.00 (4.98)	25.45 (25.40)	13.30 (13.35)
Co(NO <sub>3</sub> ) <sub>2</sub> ·6H <sub>2</sub> O 1.47	L 1.32	1:2	[Co(L) <sub>2</sub> (NO <sub>3</sub> ) <sub>2</sub> ] C <sub>6</sub> H <sub>16</sub> N <sub>10</sub> O <sub>10</sub> Co	Light Pink	446.9 [> 300]	0.18	55 [11]	16.15 (16.11)	3.64 (3.58)	31.35 (31.32)	13.20 (13.17)

16.14 corresponds to different fragments. The proposed fragmentation pattern of the bidentate ligand is given in Fig. 2.

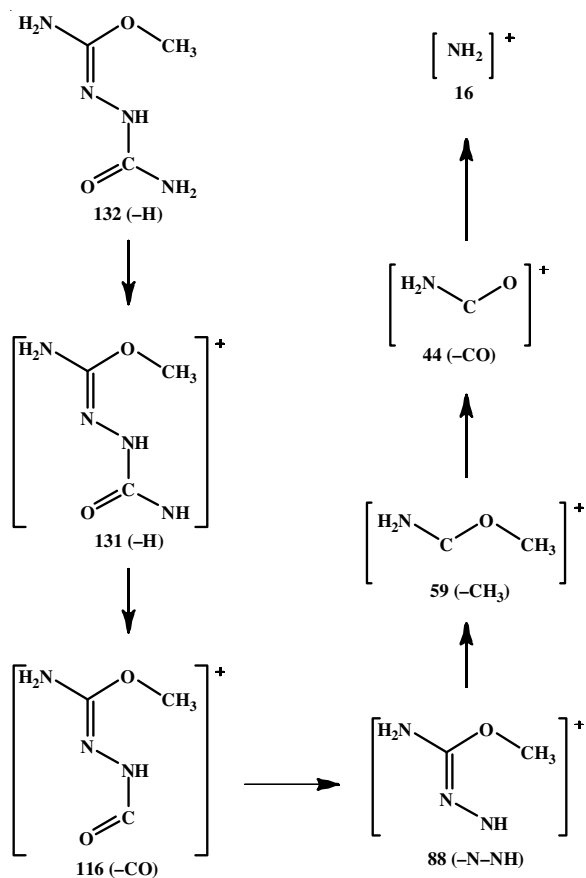


Fig. 2. Mass fragmentation pattern of methylcarbamate semicarbazone

**IR spectra:** The potential donor sites such as azomethine ( $-\text{C}=\text{N}$ ), amide group ( $-\text{CONH}_2$ ), (O) of  $\text{C}-\text{O}-\text{C}$  linkage and amino ( $-\text{NH}$ ) groups have a tendency to coordinate with metal ions. The IR spectrum of the ligand shows different bands at 3396, 3207, 1684, 1603 and  $1104\text{ cm}^{-1}$ . The strong band at  $1603\text{ cm}^{-1}$  corresponds to azomethine group of the ligand [23]. The IR spectra bands at 3396 and  $3207\text{ cm}^{-1}$  are assigned to  $-\text{NH}_2$  and  $-\text{NH}$  group respectively. The another strong intensity band at  $1104\text{ cm}^{-1}$  is due to  $\nu(\text{C}-\text{O}-\text{C})$  linkage. A sharp strong intensity band at  $1684\text{ cm}^{-1}$  is assigned to  $\nu(\text{C}=\text{O})$  of amide group [24].

The band at  $1603\text{ cm}^{-1}$  due to  $\nu(\text{C}=\text{N})$  group and  $1684\text{ cm}^{-1}$  due to  $\nu(\text{C}=\text{O})$  group shifted towards lower side after

complexation and confirms the coordination of metal ion with the nitrogen and oxygen donor atoms of the ligand [25] but the band appeared at  $1104\text{ cm}^{-1}$  due to  $\nu(\text{C}-\text{O}-\text{C})$  linkage remains unaltered suggests the non-coordination of oxygen atom. The spectra of the complexes shows the existence of a new band at  $490-430\text{ cm}^{-1}$  which may be due to  $\nu(\text{MN})$  and supports that nitrogen is coordinated [26].

**IR bands due to anions:** The existence of  $1438-1425\text{ cm}^{-1}$  and  $1315-1314\text{ cm}^{-1}$  bands in the acetato complexes with thiosemicarbazone ligand, ascribed to  $\nu_{\text{as}}(\text{OAc})$  and  $\nu_{\text{s}}(\text{OAc})$  stretching vibrations. The magnitude of  $\Delta\nu$  i.e.,  $\nu_{\text{as}}(\text{OAc})-\nu_{\text{s}}(\text{OAc})$  found to be  $110-124\text{ cm}^{-1}$ , which supported that the acetate group involved in complexation with  $\text{Mn}(\text{II})$  and  $\text{Co}(\text{II})$  ion in unidentate manner [27]. The important IR peaks of all the  $\text{Mn}(\text{II})$  and  $\text{Co}(\text{II})$  complexes are given in Table-2. The IR spectra of nitrate complexes with ligand show bands in the region of  $1412-1405\text{ cm}^{-1}$  ( $\nu_5$ ),  $1325-1304\text{ cm}^{-1}$  ( $\nu_1$ ) and  $1084-1021\text{ cm}^{-1}$  ( $\nu_2$ ). The magnitude value of  $\Delta(\nu_5-\nu_1)$  is in the range of  $87-121\text{ cm}^{-1}$  and suggests the coordination of nitrate group to the metal ions in monodentate fashion [28].

**Molar conductance:**  $\text{Mn}(\text{II})$  complexes shows the molar conductance in the range of  $0.20-0.28\ \Omega^{-1}\text{ cm}^2\text{ mol}^{-1}$  in DMSO and for  $\text{Co}(\text{II})$  complexes it lies in the range of  $0.18-0.21\ \Omega^{-1}\text{ cm}^2\text{ mol}^{-1}$  which signify the non-electrolyte character of all the metal complexes [29].

**Magnetic moment:** All the  $\text{Mn}(\text{II})$  complexes under investigation show magnetic moment in the range of  $5.84-5.96\text{ B.M}$  which corresponds to five unpaired electrons whereas  $\text{Co}(\text{II})$  complexes show in the range of  $4.73-4.82\text{ B.M}$ . (Table-3) at room temperature which corresponds to three unpaired electrons due to orbital contribution. The six coordinated octahedral geometry is assigned for all the complexes and suggested their paramagnetic behaviour [30].

**Electronic spectra:** The electronic spectra of  $\text{Mn}(\text{II})$  complexes was recorded in DMSO solution. The four absorption bands appeared in the range of  $17331-18727\text{ cm}^{-1}$ ,  $20877-21459\text{ cm}^{-1}$ ,  $26178-28480\text{ cm}^{-1}$  and  $33223-37453\text{ cm}^{-1}$  may be due to the transitions,  ${}^6\text{A}_{1g} \rightarrow {}^4\text{T}_{1g}$  ( ${}^4\text{G}$ ),  ${}^6\text{A}_{1g} \rightarrow {}^4\text{E}_g$ ,  ${}^4\text{A}_{1g}$  ( ${}^4\text{G}$ ),  ${}^6\text{A}_{1g} \rightarrow {}^4\text{E}_g$  ( ${}^4\text{D}$ ) and  ${}^6\text{A}_{1g} \rightarrow {}^4\text{T}_{1g}$  ( ${}^4\text{P}$ ), respectively. The obtained transitions discovered that  $\text{Mn}(\text{II})$  complexes have an octahedral geometry [31].

Electronic spectra of  $\text{Co}(\text{II})$  complexes showed bands in the range of  $9728-9804\text{ cm}^{-1}$ ,  $12579-12870\text{ cm}^{-1}$  and  $18999-19724\text{ cm}^{-1}$  which may be assigned to the transitions,  ${}^4\text{T}_{1g} \rightarrow {}^4\text{T}_{2g}$  (F),  ${}^4\text{T}_{1g} \rightarrow {}^4\text{A}_{2g}$  (F) and  ${}^4\text{T}_{1g} \rightarrow {}^4\text{T}_{1g}$  (P), respectively.

TABLE-2  
IR PEAKS OF SEMICARBAZONE AND ITS METAL COMPLEXES

Compounds	Assignments ( $\text{cm}^{-1}$ )					Bands due to anions
	$\nu(\text{C}=\text{N})$	$\nu(\text{C}=\text{O})$	$\nu(\text{C}-\text{O}-\text{C})$	$\nu(\text{Co} \leftarrow \text{O})$	$\nu(\text{Co} \leftarrow \text{N})$	
Ligand L	1603	1684	1104	–	–	–
$[\text{Mn}(\text{L})_2(\text{OAc})_2]$	1601	1661	1104	564	490	$\nu_{\text{as}}(\text{OAc}) = 1425\text{ cm}^{-1}$ and $\nu_{\text{s}}(\text{OAc}) = 1315\text{ cm}^{-1}$ , $\Delta\nu = 110\text{ cm}^{-1}$ indicates the monodentate nature of acetato group
$[\text{Mn}(\text{L})_2(\text{NO}_3)_2]$	1589	1678	1104	572	486	$\nu_5 = 1412\text{ cm}^{-1}$ , $\nu_1 = 1325\text{ cm}^{-1}$ and $\nu_2 = 1021\text{ cm}^{-1}$ , $\Delta\nu = 87\text{ cm}^{-1}$ indicates the monodentate nature of nitrate group
$[\text{Co}(\text{L})_2(\text{OAc})_2]$	1558	1649	1104	547	432	$\nu_{\text{as}}(\text{OAc}) = 1438\text{ cm}^{-1}$ and $\nu_{\text{s}}(\text{OAc}) = 1314\text{ cm}^{-1}$ , $\Delta\nu = 124\text{ cm}^{-1}$ indicates the monodentate nature of acetato group
$[\text{Co}(\text{L})_2(\text{NO}_3)_2]$	1577	1647	1104	585	435	$\nu_5 = 1405\text{ cm}^{-1}$ , $\nu_1 = 1304\text{ cm}^{-1}$ and $\nu_2 = 1084\text{ cm}^{-1}$ , $\Delta\nu = 121\text{ cm}^{-1}$ indicates the monodentate nature of nitrate group

TABLE-3  
MAGNETIC MOMENT, ELECTRONIC SPECTRA DATA AND LIGAND FIELD PARAMETERS OF METAL COMPLEXES

Complexes	$\mu_{\text{eff}}$ (B.M.)	Electronic transition				Ligand field parameters							
		$\lambda_{\text{max}}$ (cm <sup>-1</sup> )				Dq (cm <sup>-1</sup> )	B (cm <sup>-1</sup> )	C (cm <sup>-1</sup> )	$\beta$	F <sub>2</sub>	F <sub>4</sub>	hx	LFSE (KJ/mol)
[Mn(L) <sub>2</sub> (OAc) <sub>2</sub> ]	5.96	17331	20877	28490	33223	1733	316	3544	0.40	822	101	8.5	–
[Mn(L) <sub>2</sub> (NO <sub>3</sub> ) <sub>2</sub> ]	5.84	18727	21459	26178	37453	1873	238	3816	0.30	783	109	10	–
[Co(L) <sub>2</sub> (OAc) <sub>2</sub> ]	4.73	9728	12579	19724	35587	973	1013	–	0.90	–	–	–	93.09
[Co(L) <sub>2</sub> (NO <sub>3</sub> ) <sub>2</sub> ]	4.82	9804	12870	18999	36783	980	1021	–	0.91	–	–	–	93.82

The electronic spectra of Co(II) complexes also showed bands in the range of 35587–36783 cm<sup>-1</sup> which are due to the charge transfer [32]. The octahedral geometry was suggested around the Co(II) ion depending on the position of bands [33]. The data of electronic spectra and ligand field parameters of complexes are listed in Table-3.

**Electron paramagnetic resonance spectra:** The EPR spectra of Mn(II) complexes in polycrystalline form at liquid nitrogen temperature on X band at a frequency of 9.1 GHz and the magnetic-field strength of 3000 G. It results in the value of electron spin-nuclear spin hyperfine coupling constant ( $g_{\text{iso}}$ ) = 1.95–2.08. It was found that the signals in the polycrystalline form are too broad to be detectable. These confirmed the strong coupling of spin-system to the lattice vibrations and small spin relaxation [34]. The values of  $g_{\text{iso}}$  were evaluated by taking the average of all observed lines and found to possess an octahedral environment.

The values of  $g_{\text{iso}}$  were found to be lower than the pure compound which clearly indicates the covalent nature of the metal-ligand bond.

The electron paramagnetic resonance spectra of Co(II) complexes were studied in polycrystalline form at room temperature. The X-band EPR spectra of Co(II) complexes shows the broad signal with the values  $g_{\text{H}}$  = 2.20–3.42,  $g_{\text{L}}$  = 1.86–2.71 and  $g_{\text{iso}}$  = 1.91–2.95. The values of  $g$  confirms the octahedral environment around Co(II) complexes [35,36]. The EPR signal of polycrystalline powder for Co(II) complexes are broad and the width of the bands depended on the temperature. The EPR signals are observed only at low temperature because of the fast spin-relaxation time of high spin Co(II) ion. On the other hand, the  $g$ -values are independent of temperature. The X-band EPR spectra are consistent with a  $S=3/2$  spin state. As it is hard to resolve this splitting in magnetically diluted Co(II) complexes, so no hyperfine splitting of the transition is observed [37]. The values of  $g_{\text{iso}}$  for the Mn(II) complexes and the values of  $g_{\text{H}}$ ,  $g_{\text{L}}$  and  $g_{\text{iso}}$  for Co(II) complexes are given in Table-4.

TABLE-4  
ELECTRON PARAMAGNETIC RESONANCE  
SPECTRA DATA OF METAL COMPLEXES

Complexes	$g_{\text{H}}$	$g_{\text{L}}$	$g_{\text{iso}}$
[Mn(L) <sub>2</sub> (OAc) <sub>2</sub> ]	–	–	2.04
[Mn(L) <sub>2</sub> (NO <sub>3</sub> ) <sub>2</sub> ]	–	–	1.97
[Co(L) <sub>2</sub> (OAc) <sub>2</sub> ]	2.31	2.03	2.12
[Co(L) <sub>2</sub> (NO <sub>3</sub> ) <sub>2</sub> ]	2.28	1.77	1.94

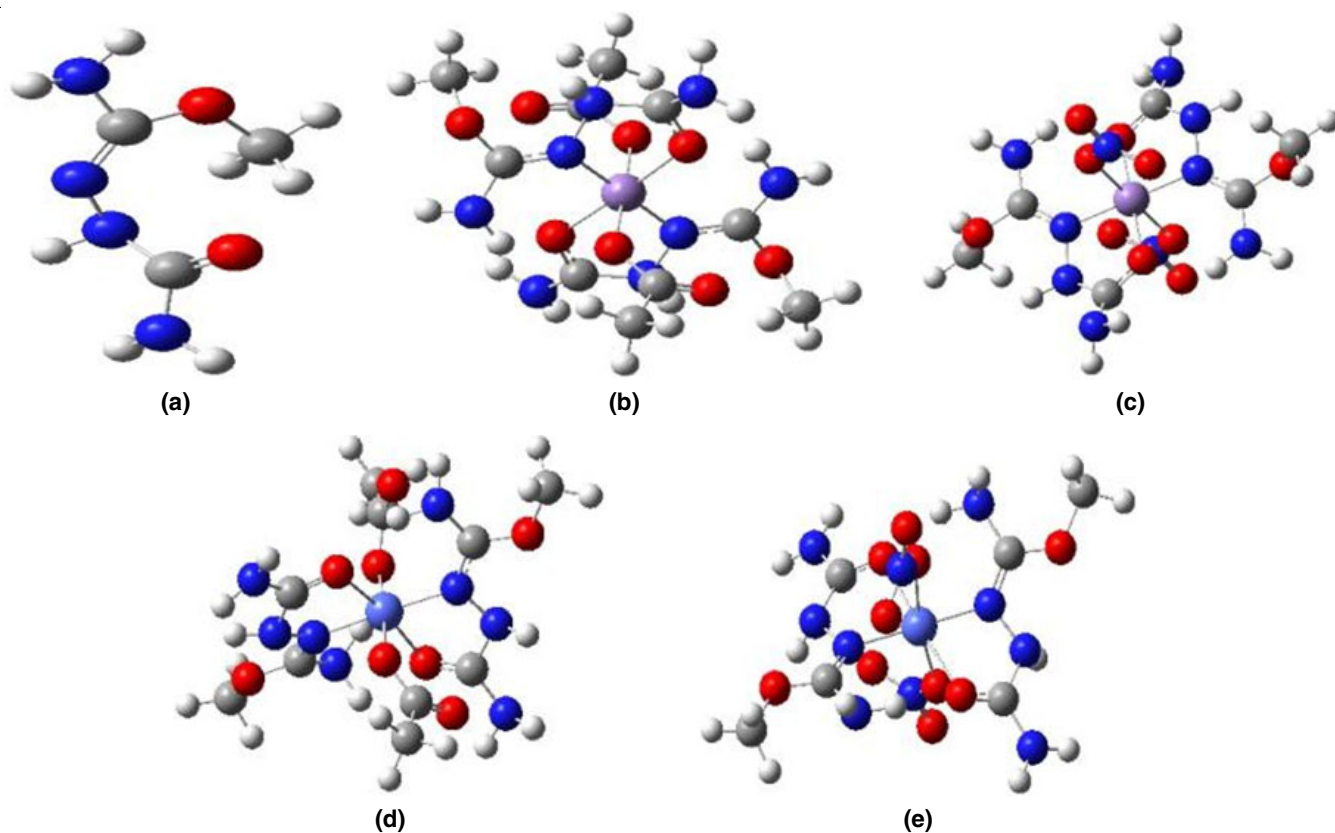
**Molecular modeling analysis:** Geometric optimization was carried out with the objective of obtaining structural information for the ligand, Mn(II) and Co(II) complexes of semi-

carbazone bidentate ligand. Semiempirical (PM6) method of the Gaussian 09 W package in the gas phase is used for the optimization of the ligand and complexes. The actual bond lengths and bond angles of molecule are evaluated by molecular modeling analysis [38]. The complete optimized geometry of the bidentate ligand and its metal complexes are shown in Fig. 3.

In [Mn(L)<sub>2</sub>(OAc)<sub>2</sub>] and [Co(L)<sub>2</sub>(OAc)<sub>2</sub>] complexes, both the axial positions are occupied by O-atom of OAc<sup>-</sup> ions whereas in [Mn(L)<sub>2</sub>(NO<sub>3</sub>)<sub>2</sub>] and [Co(L)<sub>2</sub>(NO<sub>3</sub>)<sub>2</sub>] complexes, these are occupied by O-atom of NO<sub>3</sub><sup>-</sup> ions respectively. The two equatorial positions are occupied by N-atoms of C=N group and other two are engaged by O-atoms of C=O group of ligands. The axial distance values of Mn-X<sub>19</sub> and Mn-X<sub>20</sub> (X= OAc<sup>-</sup>, NO<sub>3</sub><sup>-</sup>) for [Mn(L)<sub>2</sub>(OAc)<sub>2</sub>] are 1.975 Å, 1.936 Å and for [Mn(L)<sub>2</sub>(NO<sub>3</sub>)<sub>2</sub>] the values are 2.990 Å, 2.991 Å, respectively. The distances of bond for [Mn(L)<sub>2</sub>(OAc)<sub>2</sub>] at four equatorial positions having C=N and C=O bonds are 1.979 Å, 1.950 Å, 1.894 Å, 1.909 Å whereas for [Mn(L)<sub>2</sub>(NO<sub>3</sub>)<sub>2</sub>] the distances are 1.947 Å, 1.947 Å, 1.898 Å, 1.898 Å. The bond angles of N<sub>14</sub>-Mn<sub>21</sub>-X<sub>20</sub>, O<sub>9</sub>-Mn<sub>21</sub>-X<sub>20</sub>, N<sub>5</sub>-Mn<sub>21</sub>-X<sub>19</sub> and O<sub>10</sub>-Mn<sub>21</sub>-X<sub>19</sub> for [Mn(L)<sub>2</sub>(OAc)<sub>2</sub>] are found to be 97.322°, 98.134°, 97.028° and 85.206° respectively and for [Mn(L)<sub>2</sub>(NO<sub>3</sub>)<sub>2</sub>], the bond angles are 94.400°, 70.750°, 82.814° and 93.171° respectively.

The axial distance of Co-X<sub>19</sub> and Co-X<sub>20</sub> (X= OAc<sup>-</sup>, NO<sub>3</sub><sup>-</sup>) for [Co(L)<sub>2</sub>(OAc)<sub>2</sub>] are found to be 1.972 Å, 1.983 Å and in case of [Co(L)<sub>2</sub>(NO<sub>3</sub>)<sub>2</sub>] the values are 1.989 Å, 1.977 Å, respectively. The distances of bond at four equatorial positions containing Co<sub>21</sub>-O<sub>9</sub>, Co<sub>21</sub>-O<sub>10</sub>, Co<sub>21</sub>-N<sub>5</sub> and Co<sub>21</sub>-N<sub>14</sub> bonds are 2.153 Å, 2.176 Å, 1.918 Å and 1.909 Å, respectively in case of [Co(L)<sub>2</sub>(OAc)<sub>2</sub>] whereas the corresponding values for [Co(L)<sub>2</sub>(NO<sub>3</sub>)<sub>2</sub>] are 2.140 Å, 2.184 Å, 1.920 Å and 1.926 Å, respectively. The bond angles, O<sub>10</sub>-Co<sub>21</sub>-N<sub>14</sub> and O<sub>9</sub>-Co<sub>21</sub>-N<sub>5</sub> for [Co(L)<sub>2</sub>(OAc)<sub>2</sub>] in the equatorial plane of the coordination sphere are found to be 78.443°, 80.157° and for [Co(L)<sub>2</sub>(NO<sub>3</sub>)<sub>2</sub>], the bond angles are 76.522°, 78.954°. The slight distortion from a regular octahedral geometry of these complexes results in deviations in the bond angles in the coordination sphere. According to the calculated bond lengths and bond angles, all the Mn(II) and Co(II) complexes are found to demonstrate six coordinated octahedral geometry with slight distortion [39]. The calculated bond lengths and bond angles of ligand and complexes are shown in Tables 5 and 6.

**Antibacterial activity:** Well diffusion method was employed to evaluate the antibacterial activity of Schiff's base ligand and its complexes [40] against *S. aureus* and *P. aeruginosa* bacteria. DMSO was employed to get the different concentrations *i.e.*, 1000, 750, 500 and 250 ppm of the test compounds.



[Colour Code: C-Dark grey, H-Light grey, N-Dark blue, O-Red, Co-Light blue, Mn-purple]

Fig. 3. Optimized structure of Schiff's base ligand and metal complexes (a) Ligand, (b)  $[\text{Mn}(\text{L})_2(\text{OAc})_2]$ , (c)  $[\text{Mn}(\text{L})_2(\text{NO}_3)_2]$ , (d)  $[\text{Co}(\text{L})_2(\text{OAc})_2]$ , (e)  $[\text{Co}(\text{L})_2(\text{NO}_3)_2]$

TABLE-5  
BOND LENGTH IN ANGSTROM FOR OPTIMIZED GEOMETRY OF LIGAND AND COMPLEXES

Bond length	Ligand L	$[\text{Mn}(\text{L})_2(\text{OAc})_2]$	$[\text{Mn}(\text{L})_2(\text{NO}_3)_2]$	$[\text{Co}(\text{L})_2(\text{OAc})_2]$	$[\text{Co}(\text{L})_2(\text{NO}_3)_2]$
C <sub>1</sub> -O <sub>2</sub>	1.450	1.464	1.461	1.457	1.458
C <sub>3</sub> -O <sub>2</sub>	1.376	1.394	1.393	1.372	1.367
C <sub>3</sub> -N <sub>4</sub>	1.412	1.389	1.387	1.415	1.413
C <sub>3</sub> -N <sub>5</sub>	1.322	1.339	1.337	1.332	1.336
N <sub>5</sub> -N <sub>6</sub>	1.400	1.395	1.408	1.412	1.419
C <sub>7</sub> -N <sub>6</sub>	1.450	1.435	1.446	1.446	1.448
C <sub>7</sub> -N <sub>8</sub>	1.406	1.411	1.431	1.411	1.384
C <sub>7</sub> -O <sub>9</sub>	1.219	1.313	1.321	1.247	1.245
C <sub>12</sub> -O <sub>10</sub>	—	1.317	1.320	1.233	1.241
C <sub>12</sub> -N <sub>11</sub>	—	1.437	1.431	1.402	1.380
C <sub>12</sub> -N <sub>13</sub>	—	1.440	1.446	1.442	1.458
N <sub>13</sub> -N <sub>14</sub>	—	1.413	1.409	1.405	1.422
C <sub>15</sub> -N <sub>14</sub>	—	1.332	1.337	1.326	1.341
C <sub>15</sub> -N <sub>16</sub>	—	1.387	1.386	1.424	1.412
C <sub>15</sub> -O <sub>17</sub>	—	1.392	1.393	1.373	1.363
C <sub>18</sub> -O <sub>17</sub>	—	1.461	1.461	1.460	1.459
M <sub>21</sub> -O <sub>9</sub>	—	1.979	1.947	2.153	2.140
M <sub>21</sub> -O <sub>10</sub>	—	1.950	1.947	2.176	2.184
M <sub>21</sub> -N <sub>5</sub>	—	1.894	1.898	1.918	1.920
M <sub>21</sub> -N <sub>14</sub>	—	1.909	1.898	1.909	1.926
M <sub>21</sub> -X <sub>19</sub>	—	1.957	2.990	1.972	1.989
M <sub>21</sub> -X <sub>20</sub>	—	1.936	2.991	1.983	1.977

The antibacterial screening data demonstrate that both the ligand and metal complexes possess antibacterial properties. The more inhibitory action was found in metal complexes as compared to parent ligand. Overtone's concept and chelation

theory explains this activity enhancement of the free ligand after the complexation with metal ion [41].

Basically, the metal ion charge is decreased to a minimum, increases the lipophilicity of the complexes. This breaks the

TABLE-6  
BOND ANGLE IN DEGREE FOR OPTIMIZED GEOMETRY OF LIGAND AND COMPLEXES

Bond length	Ligand L	[Mn(L) <sub>2</sub> (OAc) <sub>2</sub> ]	[Mn(L) <sub>2</sub> (NO <sub>3</sub> ) <sub>2</sub> ]	[Co(L) <sub>2</sub> (OAc) <sub>2</sub> ]	[Co(L) <sub>2</sub> (NO <sub>3</sub> ) <sub>2</sub> ]
C <sub>1</sub> -O <sub>2</sub> -C <sub>3</sub>	119.718	113.465	116.458	118.333	118.688
O <sub>2</sub> -C <sub>3</sub> -N <sub>4</sub>	105.871	112.832	110.773	119.509	119.666
O <sub>2</sub> -C <sub>3</sub> -N <sub>5</sub>	136.020	121.199	124.861	117.146	117.669
N <sub>4</sub> -C <sub>3</sub> -N <sub>5</sub>	118.080	125.027	120.860	123.082	122.256
C <sub>3</sub> -N <sub>5</sub> -N <sub>6</sub>	122.079	118.326	116.947	117.802	116.465
N <sub>5</sub> -N <sub>6</sub> -C <sub>7</sub>	115.107	112.989	113.541	110.443	109.656
N <sub>6</sub> -C <sub>7</sub> -N <sub>8</sub>	115.600	115.906	116.846	116.749	116.972
N <sub>6</sub> -C <sub>7</sub> -O <sub>9</sub>	123.408	124.147	123.157	119.884	120.876
N <sub>8</sub> -C <sub>7</sub> -O <sub>9</sub>	—	119.895	119.995	121.632	121.729
C <sub>18</sub> -O <sub>17</sub> -C <sub>15</sub>	—	117.563	118.187	117.954	118.984
O <sub>17</sub> -C <sub>15</sub> -N <sub>16</sub>	—	115.482	115.784	118.672	119.186
O <sub>17</sub> -C <sub>15</sub> -N <sub>14</sub>	—	120.815	121.778	117.195	118.807
N <sub>16</sub> -C <sub>15</sub> -N <sub>14</sub>	—	115.566	114.972	124.101	121.412
C <sub>15</sub> -N <sub>14</sub> -N <sub>13</sub>	—	120.335	119.588	119.718	116.577
N <sub>14</sub> -N <sub>13</sub> -C <sub>12</sub>	—	114.072	113.763	110.768	108.629
N <sub>13</sub> -C <sub>12</sub> -O <sub>10</sub>	—	121.898	122.562	120.914	120.198
N <sub>13</sub> -C <sub>12</sub> -N <sub>11</sub>	—	115.895	116.122	176.222	116.692
N <sub>11</sub> -C <sub>12</sub> -O <sub>10</sub>	—	121.690	120.849	122.863	123.007
O <sub>10</sub> -M <sub>21</sub> -N <sub>14</sub>	—	89.508	90.754	78.443	76.522
O <sub>9</sub> -M <sub>21</sub> -N <sub>5</sub>	—	87.486	87.284	80.157	78.954
N <sub>14</sub> -M <sub>21</sub> -X <sub>20</sub>	—	97.322	94.400	89.697	83.842
O <sub>9</sub> -M <sub>21</sub> -X <sub>20</sub>	—	98.134	70.750	102.677	107.577
N <sub>5</sub> -M <sub>21</sub> -X <sub>19</sub>	—	97.028	82.814	93.469	95.508
O <sub>10</sub> -M <sub>21</sub> -X <sub>19</sub>	—	85.206	93.171	108.688	108.114
X <sub>19</sub> -M <sub>21</sub> -X <sub>20</sub>	—	178.504	174.202	175.191	169.394

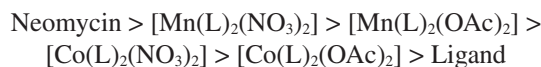
TABLE-7  
ANTIBACTERIAL ACTIVITY DATA OF  
LIGAND AND COMPLEXES SHOWING ZONE OF  
INHIBITION (mm) AT 250, 500, 750 AND 1000 ppm

Compound	Concentration (ppm)	Zone of inhibition (mm)	
		<i>S. aureus</i>	<i>P. aeruginosa</i>
Ligand	1000	15	12
	750	12	10
	500	11	8
	250	8	6
[Mn(L) <sub>2</sub> (OAc) <sub>2</sub> ]	1000	25	18
	750	20	16
	500	18	14
	250	12	12
[Mn(L) <sub>2</sub> (NO <sub>3</sub> ) <sub>2</sub> ]	1000	30	15
	750	28	12
	500	24	11
	250	20	10
[Co(L) <sub>2</sub> (OAc) <sub>2</sub> ]	1000	21	26
	750	20	19
	500	18	17
	250	14	15
[Co(L) <sub>2</sub> (NO <sub>3</sub> ) <sub>2</sub> ]	1000	25	20
	750	21	18
	500	18	17
	250	15	16
Neomycin	1000	34	31
	750	30	27
	500	29	25
	250	26	22

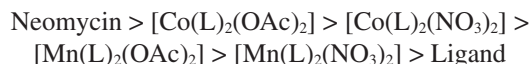
permeability barrier of the cell and hence retards the cell processes. Principally the complex with increased lipophilic character favours its access through the cell membrane's lipid layer and blocks the site of metal binding in the enzymes of

microorganisms. As a result of which the respiration of the cell get disturbs and breaks the chain of protein synthesis [42]. On the basis of screening data (Table-7), it can also be said that the inhibition action increases with increase in concentration [43].

The order of antibacterial activity for *S. aureus* was found to be:



The order of antibacterial activity for *P. aeruginosa* was found to be:



#### ACKNOWLEDGEMENTS

One of the authors, Pallavi Jain is thankful to Prof. Manoj Kumar Pandey, Director, SRM Institute of Science & Technology, Modinagar, India for providing research facilities and constant encouragements. The authors are also thankful to IIT Bombay, Mumbai, India for recording EPR spectra, IIT Delhi, Delhi, India for recording NMR, Mass and IR spectra.

#### REFERENCES

1. M. Arockia doss, S. Savithiri, G. Rajarajan, V. Thanikachalam and H. Saleem, *Spectrochim. Acta A Mol. Biomol. Spectrosc.*, **148**, 189 (2015); <https://doi.org/10.1016/j.saa.2015.03.117>.
2. S. Farhadi, F. Mahmoudi and J. Simpson, *J. Mol. Struct.*, **1108**, 583 (2016); <https://doi.org/10.1016/j.molstruc.2015.12.038>.
3. T.K. Venkatachalam, P.V. Bernhardt, C.J. Noble, N. Fletcher, G.K. Pierens, K.J. Thurecht and D.C. Reutens, *J. Inorg. Biochem.*, **162**, 295 (2016); <https://doi.org/10.1016/j.jinorgbio.2016.04.006>.
4. A.A. Jadhav, V.P. Dhanwe and P.K. Khanna, *Polyhedron*, **123**, 99 (2017); <https://doi.org/10.1016/j.poly.2016.10.039>.

5. A.A. Fesenko, A.N. Yankov and A.D. Shutalev, *Tetrahedron Lett.*, **57**, 5784 (2016); <https://doi.org/10.1016/j.tetlet.2016.11.041>.
6. H. Chen, X. Ma, Y. Lv, L. Jia, J. Xu, Y. Wang and Z. Ge, *J. Mol. Struct.*, **1109**, 146 (2016); <https://doi.org/10.1016/j.molstruc.2015.12.014>.
7. R.J. Kunnath, M. Sithambaresan, A.A. Aravindakshan, A. Natarajan and M.R.P. Kurup, *Polyhedron*, **113**, 73 (2016); <https://doi.org/10.1016/j.poly.2016.04.003>.
8. M.J. Ahsan, M. Amir, M.A. Bakht, J.G. Samy, M.Z. Hasan and M.S. Nomani, *Arab. J. Chem.*, **9**, S861 (2016); <https://doi.org/10.1016/j.arabjc.2011.09.012>.
9. C. Gan, J. Cui, S. Su, Q. Lin, L. Jia, L. Fan and Y. Huang, *Steroids*, **87**, 99 (2014); <https://doi.org/10.1016/j.steroids.2014.05.026>.
10. Z. Liu, S. Wu, Y. Wang, R. Li, J. Wang, L. Wang, Y. Zhao and P. Gong, *Eur. J. Med. Chem.*, **87**, 782 (2014); <https://doi.org/10.1016/j.ejmech.2014.10.022>.
11. E.A. Enyedy, G.M. Bogнар, N.V. Nagy, T. Jakusch, T. Kiss and D. Gambino, *Polyhedron*, **67**, 242 (2014); <https://doi.org/10.1016/j.poly.2013.08.053>.
12. S.M.M. Ali, M. Jesmin, M.A.K. Azad, M.K. Islam and R. Zahan, *Asian Pac. J. Trop. Biomed.*, **2**, S1036 (2012); [https://doi.org/10.1016/S2221-1691\(12\)60357-8](https://doi.org/10.1016/S2221-1691(12)60357-8).
13. K. Alomar, V. Gaumet, M. Allain, G. Bouet and A. Landreau, *J. Inorg. Biochem.*, **115**, 36 (2012); <https://doi.org/10.1016/j.jinorgbio.2012.04.022>.
14. R.B. de Oliveira, E.M. de Souza-Fagundes, R.P.P. Soares, A.A. Andrade, A.U. Krettlі and C.L. Zani, *Eur. J. Med. Chem.*, **43**, 1983 (2008); <https://doi.org/10.1016/j.ejmech.2007.11.012>.
15. M.A. Alves, A.C. de Queiroz, M.S. Alexandre-Moreira, J. Varela, H. Cerecetto, M. González, A.C. Doriguetto, I.M. Landre, E.J. Barreiro and L.M. Lima, *Eur. J. Med. Chem.*, **100**, 24 (2015); <https://doi.org/10.1016/j.ejmech.2015.05.046>.
16. L.C. Dias, G.M. de Lima, C.B. Pinheiro, B.L. Rodrigues, C.L. Donnici, R.T. Fujiwara, D.C. Bartholomeu, R.A. Ferreira, S.R. Ferreira, T.A.O. Mendes, J.G. da Silva and M.R.A. Alves, *J. Mol. Struct.*, **1079**, 298 (2015); <https://doi.org/10.1016/j.molstruc.2014.08.047>.
17. G. Scalese, J. Benitez, S. Rostan, I. Correia, L. Bradford, M. Vieites, L. Minini, A. Merlino, E.L. Coitino, E. Birriel, J. Varela, H. Cerecetto, M. Gonzalez, J.C. Pessoa and D. Gambino, *J. Inorg. Biochem.*, **147**, 116 (2015); <https://doi.org/10.1016/j.jinorgbio.2015.03.002>.
18. X. Jiang, L. Sheng, C. Song, N. Du, H. Xu, Z. Liu and S. Chen, *New J. Chem.*, **40**, 3520 (2016); <https://doi.org/10.1039/C5NJ01601K>.
19. X. Zhai, G. Bao, L. Wang, M. Cheng, M. Zhao, S. Zhao, H. Zhou and P. Gong, *Bioorg. Med. Chem.*, **24**, 1331 (2016); <https://doi.org/10.1016/j.bmc.2016.02.003>.
20. N. Raghav and R. Kaur, *Int. J. Biol. Macromol.*, **80**, 710 (2015); <https://doi.org/10.1016/j.ijbiomac.2015.07.029>.
21. S. Chandra, K. Sharma and A. Kumar, *J. Saudi Chem. Soc.*, **18**, 555 (2014); <https://doi.org/10.1016/j.jscs.2011.11.002>.
22. P. Goel, D. Kumar, S. Chandra and A. Kumar, *Iran. J. Sci. Technol. Trans. Sci.*, **42**, 557 (2018); <https://doi.org/10.1007/s40995-016-0140-6>.
23. M. Tyagi and S. Chandra, *J. Saudi Chem. Soc.*, **18**, 53 (2014); <https://doi.org/10.1016/j.jscs.2011.05.013>.
24. H.L. Singh, J.B. Singh and S. Bhanuka, *J. Coord. Chem.*, **69**, 343 (2016); <https://doi.org/10.1080/00958972.2015.1115485>.
25. H.F.A. El-halim, M.M. Omar, G.G. Mohamed, M.A.E. Sayed, *Eur. J. Chem.*, **2**, 178 (2011); <https://doi.org/10.5155/eurjchem.2.2.178-188.240>.
26. G. Mahmoudi, A. Castineiras, P. Garczarek, A. Bauza, A.L. Rheingold, V. Kinzhybalо and A. Frontera, *CrystEngComm*, **18**, 1009 (2016); <https://doi.org/10.1039/C5CE02371H>.
27. S. Chandra and L.K. Gupta, *Spectrochim. Acta A Mol. Biomol. Spectrosc.*, **61**, 2549 (2005); <https://doi.org/10.1016/j.saa.2004.08.028>.
28. D. Shukla, L.K. Gupta and S. Chandra, *Spectrochim. Acta A Mol. Biomol. Spectrosc.*, **71**, 746 (2008); <https://doi.org/10.1016/j.saa.2007.12.052>.
29. P. Tyagi, S. Chandra, B.S. Saraswat and D. Sharma, *Spectrochim. Acta A Mol. Biomol. Spectrosc.*, **143**, 1 (2015); <https://doi.org/10.1016/j.saa.2015.02.027>.
30. S.A. Aly, *J. Radiat. Res. Appl. Sci.*, (2017); <http://doi.org/10.1016/j.jrras.2017.04.001>.
31. T.A. El-Karim and A.A. El-Sherif, *J. Mol. Liq.*, **219**, 914 (2016); <https://doi.org/10.1016/j.molliq.2016.04.005>.
32. I. Babahan, F. Eyduran, E.P. Coban, N. Orhan, D. Kazar and H. Biyik, *Spectrochim. Acta A Mol. Biomol. Spectrosc.*, **121**, 205 (2014); <https://doi.org/10.1016/j.saa.2013.10.040>.
33. M. Sobiesiak, T. Muziol, M. Rozalski, U. Krajewska and E. Budzisz, *New J. Chem.*, **38**, 5349 (2014); <https://doi.org/10.1039/C4NJ00977K>.
34. S. Verma, S. Chandra, U. Dev and N. Joshi, *Spectrochim. Acta A Mol. Biomol. Spectrosc.*, **74**, 370 (2009); <https://doi.org/10.1016/j.saa.2009.06.029>.
35. S. Chandra and A. Kumar, *Spectrochim. Acta A Mol. Biomol. Spectrosc.*, **67**, 697 (2007); <https://doi.org/10.1016/j.saa.2006.07.051>.
36. R. Marts, J.C. Kaine, R.R. Baum, V.L. Clayton, J.R. Bennett, L.J. Cordonnier, R. McCarrick, A. Hasheminasab, L.A. Crandall, C.J. Ziegler and D.L. Tierney, *Inorg. Chem.*, **56**, 618 (2017); <https://doi.org/10.1021/acs.inorgchem.6b02520>.
37. G. Schmidt, W.S. Brey Jr. and R.C. Stoufer, *Inorg. Chem.*, **6**, 268 (1967); <https://doi.org/10.1021/ic50048a016>.
38. M. Tyagi, S. Chandra and P. Tyagi, *Spectrochim. Acta A Mol. Biomol. Spectrosc.*, **117**, 1 (2014); <https://doi.org/10.1016/j.saa.2013.07.074>.
39. S. Chandra, S. Bargujar, R. Nirwal, K. Qanungo and S.K. Sharma, *Spectrochim. Acta A Mol. Biomol. Spectrosc.*, **113**, 164 (2013); <https://doi.org/10.1016/j.saa.2013.04.114>.
40. C. Perez, M. Paul and P. Bazerque, *Acta Biol. Med. Exp.*, **15**, 113 (1990).
41. V. Prachayasittikul, V. Prachayasittikul, S. Prachayasittikul and S. Ruchirawat, *Drug Des. Devel. Ther.*, **7**, 1157 (2013); <https://doi.org/10.2147/DDDT.S49763>.
42. J.A. Gilbert and C.L. Dupont, *Annu. Rev. Mar. Sci.*, **3**, 347 (2011); <https://doi.org/10.1146/annurev-marine-120709-142811>.
43. J.L. Adrio and A.L. Demain, *Biomolecules*, **4**, 117 (2014); <https://doi.org/10.3390/biom4010117>.